

Directed Assembly of Nanoporous, Porphyrin-Based, Molecular-Square Thin Films

Undergraduate Researcher

Craig P. Schwartz, Northwestern University

Faculty Mentor

SonBinh T. Nguyen

Department of Chemistry, Northwestern University

Postdoctoral Mentor

Richard W. Gurney

Department of Materials Science and Engineering

Northwestern University

Abstract

Several phosphonate-functionalized molecular squares have been successfully synthesized, and the fabrication of multilayer films on both conductive and semiconducting platforms has been demonstrated. These films were grown using the well-documented zirconium phosphonate multilayer method. The layer-by-layer growth rate is uniform. Experiments suggest, however, that the molecular squares adopt a semi-collapsed structure upon assembling in multilayer films. Despite this structure, the films are still impermeable to molecules larger than the dimensions of an individual square cavity but highly permeable to smaller species. This research also has successfully observed a single iteration of the zirconium phosphonate multilayer assembly of the molecular square by scanning electron microscopy and atomic force microscopy through micromolding in capillary micropatterning techniques. It has demonstrated the applicability of ZPM synthesis to direct and orient larger molecular assemblies, such as nanoarchitectures, into thin-film assemblies using molecular structures with cross-sectional areas larger than have been previously reported. Furthermore, the squares were characterized by X-ray reflectivity.

Introduction

One facet of nanotechnology involves controlling the assembly of molecules to construct molecular architectures on the nanometer scale.^{1,2,3,4} An attractive method for building molecular architectures on surfaces is from the ground up via layer-by-layer directed assembly.^{5,6,7,8} The preparation of multifunctional, nanoporous thin films with uniform thicknesses and a well-defined porous structure is also desirable from a functionalized nanomaterials perspective. We envision that nanoporous thin-film materials can function as molecular sieves,^{9,10,11} frameworks for size-selective heterogeneous catalysis,¹² and chemical sensors^{13,14} and in liquid-junction solar cells¹⁵ when an appropriate chromophoric molecular framework is chosen. Recent attempts by Clearfield et al. to prepare organically pillared microporous materials yielded structures with pore sizes in the 10 to 20 Å range by cross-linking zirconium phosphate-like layers with several types of diphosphonic acids.¹⁶ This study demonstrates the applicability of the zirconium phosphonate directed assembly technique with phosphonated macrocycles having pore sizes in the 15 to 25 Å range to produce similar microporous thin-film frameworks from the surfaces of electrodes.

Novel, four-sided, box-shaped compounds called molecular squares^{17,18} were the structural starting point for this study's approach to constructing semipermeable thin films. These macromolecules have well-defined cavities of nanometer dimensions and can be easily and quantitatively synthesized via molecular directed assembly.¹⁹ In a single crystal, molecular squares typically align to form semi-

infinite, one-dimensional channels.²⁰

Further characterization of these semi-permeable materials reveals large internal surface areas and void volumes.

Molecular squares make exceptional molecular sieves demonstrating high selectivity to the size of the permeant molecule.^{21,22,23,24} In addition, porphyritic molecular squares have structurally rigid walls containing a coordinating metal center that can be further functionalized for a variety of applications, including heterogeneous catalysis and molecular sieves.^{25,26}

To obtain reproducible, robust, nanometer-thick, and semipermeable membranes featuring well-defined nanoscopic channels, a thin-film fabrication method based on zirconium phosphonate directed assembly was used^{27,28} (the same method pioneered by Mallouk,^{29,30} Katz,³¹ and Clearfield³²). The technique's success is due to the low solubility of zirconium phosphonate salts (even though both the phosphonate and zirconium precursors are highly soluble individually). Thin-film preparation via zirconium phosphonate directed assembly is highly reproducible and enables outstanding precision control over the film's thickness.³³ Due to the ease of preparation and synthesis, zirconium phosphonate multilayer (ZPM) thin films have been used for a wide variety of applications. For example, ZPMs prepared using diphosphonated oligothiophenes have been used to produce novel materials to study electron and energy transfer,^{34,35} while thin films of metal salts have been used as enantiomerically selective sensors,^{27,36} and thin films of diphosphonated asymmetric molecules have demonstrated nonlinear optical responses on the same order of magnitude of lithium niobate.^{37,38}

Theoretically, ZPMs are distinctly layered structures composed of alternating single-layer sheets of α -zirconium phosphate, separated by organic spacers and generally anchored on a floor of SiO_x or glass.³³ The layered nature of ZPM films is well established, but their structures are often presumed to be homologous with microcrystalline powders synthesized by hydrothermal methods, layers of diphosphonated organic molecules separated by single atomic sheets of the α -zirconium phosphate mineral.¹⁶ The most successful ZPM thin films have been assembled with linear, pillar-shaped molecules with cross-sectional areas less than 24 Å², because the α -zirconium phosphate sheet structure is unable to accommodate molecules with larger cross-sectional areas.³⁹ In fact, if the area is larger than 24 Å², the microcrystalline ZPM powders, synthesized through solution methods, gradually convert from a phosphonate-



Figure 1: Idealized representation of a microporous thin film with uniform thickness and a well-defined porous structure.

rich structure (2:1 -PO₃:Zr) to a phosphonate-deprived structure (1:1 -PO₃:Zr).^{16,40} Microcrystalline powders can compensate for the larger organic diphosphonates and adopt an α -zirconium phosphate bilayer structure if free phosphate ions are available in solution. Thin-film ZPMs are typically not prepared with free phosphonate ions, and one might expect that as the size of the organic diphosphonic acid spacer increases above the 24 Å² threshold, individual phosphonate-zirconium-phosphate linkages would form. In fact, a PO₃-Zr-PO₃ linkage between two large, monophosphonated crown-ethers grown hydrothermally in the presence of zirconium ions was recently determined.¹⁶

While microcrystalline zirconium phosphonate powders have been studied intensely, the structure of ZPM thin films is less understood. Specifically, little is known about the applicability of the ZPM thin-film growth technique to the field of nanotechnology and its ability to control nanoarchitecture formation.⁴¹ This research demonstrates the applicability of the zirconium phosphonate directed assembly technique to the preparation of thin films of phosphonate-functionalized porphyrins (Figure 2).⁴² In the first step toward developing nanoporous thin-film materials for a variety of applications, this study hopes to demonstrate the applicability of ZPM synthesis to direct and orient larger molecular assemblies, such as nanoarchitectures, into thin-film assemblies, as the ultimate limit of the ZPM thin-film technique using larger molecular structures with cross-sectional areas greater than 24 Å².

This report will demonstrate the synthesis and characterization of a phosphonate-functionalized molecular square and the

fabrication of multilayer films on both conducting and semiconducting platforms. The layer-by-layer ZPM growth rate is uniform; however, experiments suggest that the molecular squares adopt a semi-collapsed structure upon assembling in multilayer films. A single iteration of the ZPM assembly of the molecular square was also successfully observed using scanning electron microscopy through “micromolding in capillaries” micropatterning techniques. Most importantly, this research will demonstrate the applicability of the ZPM technique to assemble large nanostructures in a layer-by-layer fashion and the applicability of X-ray reflectivity.

Approach

For this study, 1,12-dibromododecane, (CH₃CH₂)₂PO₃, and ZrOCl₂•8 H₂O were received from Aldrich, and anhydrous-acetonitrile and H₂SO₄ were received from Fisher Scientific. 1-hexylphosphonic acid, 1-octadecylphosphonic acid, Y(NO₃)₃, and POCl₃ were received from Alfa Aesar. 3-aminopropyltrimethoxysilane (APTMS) (United Chemical Technologies, Inc.) and HfOCl₂•8 H₂O (Johnson Matthey) were used as received. 2,4,6-collidine (Acros) was dried over activated molecular sieves (4Å). 1-12-dodecane-bisphosphonic acid⁴³ was synthesized according to standard literature procedures. Ultrapure water was obtained from a Millipore filtration and ion-exchange system (resistivity of 18.2 MΩ). Single-sided InSnOx (ITO) and coated and unpolished float-glass slides (ITO thickness = 50 nm) were obtained from Delta Technologies, Ltd. (R_S = 8 - 12 Ω). *P*-type silicon <100> wafers for SEM and SIMS (thickness 256-306 μm, resistivity 1-20 Ω-cm) were purchased from Montco Silicon

Technologies, Inc. N/p/C_z type single-side polished/diced silicon <001> wafers (resistivity 1-10 Ω-cm, thickness 98-100 mils, TTV is < microns) from Umicore were used for X-ray reflectivity.

Scanning electron microscopy (SEM) measurements were performed on a Hitachi S-4500FE scanning electron microscope operating at 17 kV. Conductive carbon tape bridged the conductive surface of the ITO-coated glass slide to the conductive SEM puck, where the sample was deposited. Atomic force microscopy (AFM) measurements were performed using a Digital Instruments Bioscope AFM head and a Nanoscope IIIa controller. All measurements were obtained in contact mode with Nanoprobe SPM tips (DNP-S20, Digital Instruments).

Synthesis

For the synthesis of Diethyl-4-[12-(4-(diethoxyphosphoryl)phenyl) -21,22,23,24-tetraazapentacyclo[16.2.1.1^{3,6}.1^{8,11}.1^{13,16}] tetracosa-1(21),2,4,6,8(23),9,11,13,15,17,19-undecaen-2-yl] phenylphosphonate (1), 4.2.4-[12-(4-phosphonophenyl)-21,22,23,24-tetraazapentacyclo[16.2.1.1.1] tetracosa-1(21),2,4,6,8(23),9,11,13,15,17,19-undecaen-2-yl] phenylphosphonic acid (2), Diethyl 4-[7,17-dibromo-12-[4-(diethoxyphosphoryl)phenyl]-21,22,23,24-tetraazapentacyclo[16.2.1.1^{3,6}.1^{8,11}.1^{13,16}] tetracosa-1(21),2,4,6,8(23),9,11,13,15,17,19-undecaen-2-yl]phenylphosphonate (3), [Diethyl 4-[7,17-dibromo-12-[4-(diethoxyphosphoryl)phenyl]-21,22,23,24-tetraazapentacyclo[16.2.1.1^{3,6}.1^{8,11}.1^{13,16}] tetracosa-1(21),2,4,6,8(23),9,11,13,15,17,19-undecaen-2-yl]phenylphosphonate] zinc (II) (4), [Diethyl-4-[12-[4-(diethoxyphosphoryl)phenyl]-7,17-bis(4-pyridinylethynyl)-21,22,23,24-tetraazapentacyclo[16.2.1.1^{3,6}.1^{8,11}.1^{13,16}]

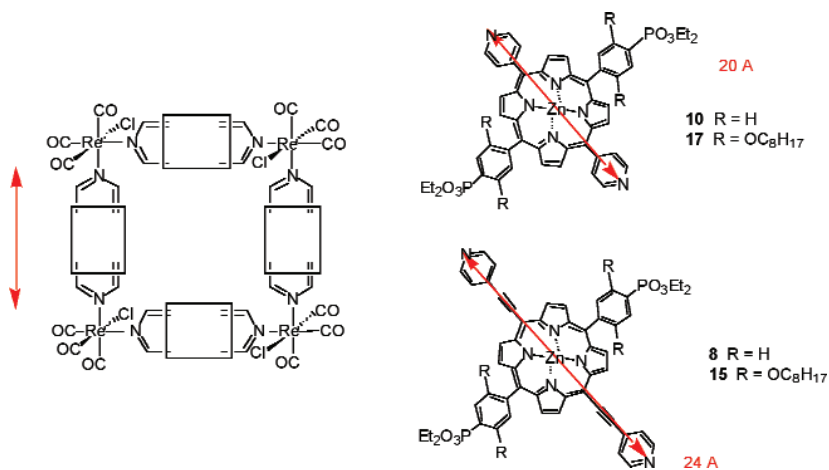


Figure 2: Schematic representation of molecular squares.

tetracosa-1(21),2,4,6,8(23),9,11,13,15,17,19-undecaen-2-yl]phenylphosphonate] zinc (II) (5), [4-[12-(4-phosphonophenyl)-7,17-bis(4-pyridinylethynyl)-21,22,23,24-tetraazapentacyclo[16.2.1.1^{3,6}.1^{8,11}.1^{13,16}] tetracosa-1(21),2,4,6,8(23),9,11,13,15,17,19-undecaen-2-yl]phenylphosphonic acid] zinc (II) (6), and [Re(CO)₃Cl]₄[5,15-Bis-4-[(pyridyl)ethynyl]-10,20-(phenyl-4-phosphonic acid)porphyrinato] zinc (II)₄ (7) see Gurney et al. (Gurney, R. W.; Paoprasert, P.; Morris, K. F.; Wightman, M. D.; Nguyen, S. T.; Hupp, J. T., personal communications.)

Thin-Film Preparation

The primary method to prepare the foundation for subsequent layer growth films was based upon the work of Horne et al. with slight modifications.^{43,44,45} The preparation works for both silicon wafers and ITO-coated glass slides, with the differences noted. In the first step, piranha solution (2:1, sulfuric acid: hydrogen peroxide) was freshly prepared (*caution:*

reacts violently with organics) and allowed to cool in an ice bath for five minutes. The substrates were then placed in the piranha solution for 10 minutes, rinsed with ultrapure water, and dried under a stream of N₂. Immediately after, the substrates were immersed in HCl (2M) for five minutes, rinsed with ultrapure water, dried under a stream of dry N₂ and oven-dried at 80°C for 15 minutes. The substrates were primed in an 80°C solution of anhydrous octanol and 3-aminopropyl-trimethoxysilane (100:1 v:v) for 10 minutes, followed by rinsing with hexanes and ultrapure water and drying under a stream of dry N₂ and in an 80°C oven for 30 minutes. To phosphorylate the sample surface, silicon substrates were placed into a mixture of POCl₃ (0.1 M) and 2,4,6-collidine (0.1 M) in anhydrous acetonitrile (ACN), for one hour. ITO-coated glass slides were only exposed to this treatment for 10 minutes. The substrates were then heated in warm, dry ACN for 15 minutes, followed by rinses

Directed Assembly of Nanoporous, Porphyrin-Based, Molecular-Square Thin Films (*continued*)

with ACN and ultrapure water. The slides were next dried under a stream of dry N_2 , placed in a solution of $ZrOCl_2 \cdot 8 H_2O$ (5 mM) for two hours, rinsed with ultrapure water, and dried under a stream of dry N_2 . The slides were then immersed in a 1 mM solution of **2** or 0.0125 mM solution of **7**, both in DMSO for two hours. The zirconation step for 30 minutes, followed by the incubation in **2**/DMSO or **7**/DMSO, was then repeated until the desired number of layers was obtained. In cases with mixed metal-ion multilayers, aqueous solutions of $HfOCl_2$ (5 mM) and $Y(NO_3)_3$ (5 mM) were used, and immersion times remained the same.

Micropatterning

The soft-lithography technique known as "micromolding in capillaries" (MIMIC) was used to obtain micropatterning of **7** and organomonophosphonates.⁴⁶ Using a previously described method,⁴⁷

polydimethylsiloxane (PDMS) stamps for microtransfer molding were fabricated by curing a 10:1 mixture of elastomer-hardener (Sylgard Silicone 184, Dow Corning) over commercially obtained lithographic master (10 μm pitch, AFM calibration grating, Digital Instruments), with etched square features approximately 185 nm deep and laterally measuring 5 x 5 μm with a lattice constant of 10 μm . The PDMS was cured at room temperature for one hour, followed by additional curing at 60°C for one hour. The PDMS stamp was placed in contact with a clean, phosphorylated, ITO-coated glass slide. An aqueous solution of $ZrOCl_2$ (5 mM) was then drawn underneath the PDMS stamp by capillary action to create a micropatterned-binding surface for **7**. After two hours, the remaining solution was carefully withdrawn from under the PDMS stamp with a μL -syringe and then flushed with several milliliters of ultrapure

water. The PDMS stamp was carefully peeled from the surface and the glass slide gently rinsed with ultrapure water and dried under a stream of dry N_2 . The micropatterned zirconium surface was then exposed to a solution of **7** in DMSO as described above or, similarly, with an organophosphonic acid (1-phenylphosphonic, 1-hexylphosphonic, and 1-octadecylphosphonic acid).

Instrumentation

X-ray reflectivity (XRR) measurements were performed at the J. B. Cohen X-Ray Diffraction Facility at Northwestern University using $Cu K\alpha$ radiation from a rotating anode line source coupled to an OSMIC MaxFlux collimating optic. A Huber slit following the collimating optic was used to define the beam size. The beam size was 0.10 x 10 mm for the lowest angular range and increased at a higher angle when it was possible to do

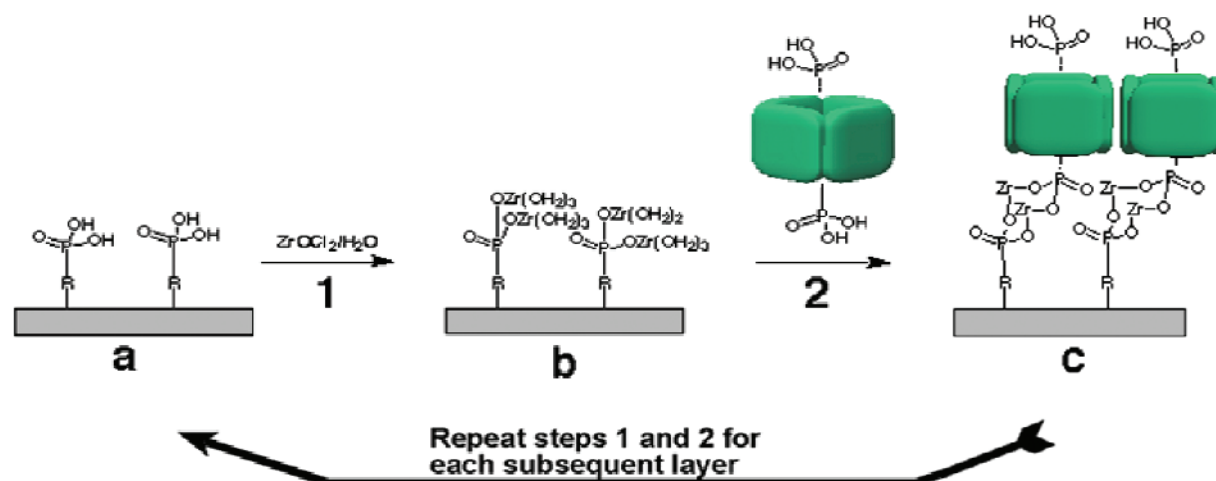


Figure 3: Layer-by-layer thin-film synthesis of **7**.

so and still fully intercept the beam with the sample. Background scans were taken on both sides of the specular condition and then averaged and subtracted from the specular data. The data was normalized to the incident beam intensity, measured before and after each scan. The reflected X-ray intensity was measured using an Oxford Cyberstar 600 scintillation counter.

Results and Discussion

Synthesis and Characterization of Phosphonated Molecular Squares

The porphyrinic molecular squares used in this study require the synthesis of orthogonally functionalized porphyrins with the 5,15 and 10,20 meso positions, containing pyridyl and phosphonate functional groups, respectively. The 5,15-meso pyridyl groups enable the formation of the molecular square through a well-documented coupling with $\text{Re}(\text{CO})_5\text{Cl}$, while the phosphonate groups in an orthogonal direction enable the preparation of thin-films of the squares via zirconium phosphonate layering (Figure 2).

Zirconium-Phosphonate

Thin-Film Assembly

Although ZPMs can be built directly on top of SiO_x substrates that are zirconated immediately after cleaning in piranha solution or after phosphorylating the piranha-cleaned substrates, the ZPMs in this study were built atop substrates primed with a foundational layer of zirconium anchored to the underlying silicon oxide substrate via a phosphorylated-aminopropyl siloxane ($\text{PO}_3\text{-APS}$), following the work of Horne et al.^{43,44,45,48} The preparation works for both silicon wafers and ITO-coated glass slides, with the differences noted in the experimental

section. The surface concentration of Zr^{2+} in the foundational layers of ZPMs prepared in this manner ranged from 1.0 to 1.6 Zr^{2+} per nm^2 from sample to sample, as determined by X-ray fluorescence yield measurements. As the concentration of hydroxyl groups on the surface of amorphous silicates has been estimated at 4.9 ($-\text{OH}$) per nm^2 ,⁴⁹ a SiO_x substrate that was fully passivated with phosphorylated-aminopropyl siloxane would have (4.9 / 3) or 1.63 Zr^{2+} per nm^2 , presuming that each aminopropyl siloxane consumes three surface hydroxyl groups, and that each surface phosphonate binds a single Zr^{2+} .

The assembly procedure for mono- and multilayer films of 7 is shown schematically in Figure 3. As porphyrins and their assemblies have large molar absorptivities, the layer-by-layer thin-film assembly of the highly chromophoric 7 was monitored by electronic absorption spectroscopy after each fabrication cycle at 448 nm, corresponding to the Soret band of 7. The deposition times for $\text{Zr}(\text{IV})$ and 7 were optimized to yield the greatest amount of 7 per assembly cycle, as indicated by electronic absorption spectroscopy. Deposition times exceeding those described in the experimental section did not lead to additional incorporation of 7. Importantly, and consistent with previous work, a subsequent layer would not deposit until the sample was exposed to a solution of $\text{Zr}(\text{IV})$; this two-step assembly sequence is the basis for systematic control of film thickness. Theoretically, repetition of this process allows for the growth of films to any number of desired layers or thickness.^{27,42}

The uptake of 7 per layer proved to be markedly dependent on the foundational layers built upon the cleaned substrates.

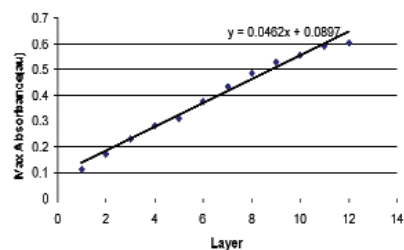


Figure 4: Monitoring of the layer-by-layer growth of a ZPM of 7 on an ITO-coated glass substrate by UV-Vis spectroscopy using a method that does not involve fixation in an oven. Note the strong deviation from linearity after 10 steps.

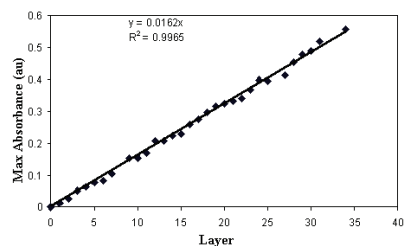


Figure 5: Monitoring of the layer-by-layer growth of a ZPM of 7 on an ITO-coated glass substrate by UV-Vis spectroscopy using the latest method.

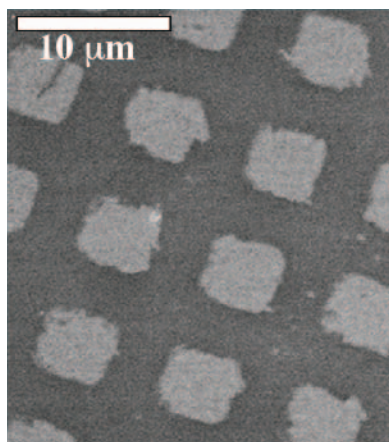


Figure 6: Scanning electron micrograph of a single iteration of a ZPM of 7 upon a Zr^{2+} micropatterned phosphorylated ITO-coated glass substrate surface. Micropatterning a single layer of 7 facilitated the observation of the film by SEM.

When the method for film growth detailed in the procedure was performed without the steps involving the oven film, growth deviated strongly from linearity in a rapid format, particularly preceding layer 10 (Figure 4). However, when the oven steps were added, adsorption of 7 was demonstrated to be consistently linear through 35 layers (Figure 5).

The measured absorbance intensity for a ZPM of 7 increased at a rate of 0.008 absorbance units per layer, resulting in a calculated density of 0.05 squares/nm². The theoretical density, assuming a densely packed square structure on the surface not considering van der Waals radii, is $1/(2.4 \text{ nm})^2$ or 0.088 squares/nm², giving a film coverage of 57% of a closely packed monolayer of square.

To directly observe a single iteration of the ZPM directed-assembly of 7 through SEM, Zr^{2+} was micropatterned on a phosphorylated ITO-coated glass substrate and then introduced to a solution of 7. As expected, the region of the substrate terminated in 7 is comparatively less conductive and, therefore, darker in the SEM image in comparison with the Zr -terminated regions and different in heights by AFM (Figures 6 and 7, respectively). Micropatterning a single layer of 7 facilitated the observation of the film by SEM and AFM. Subsequent layers were not grown atop this single-micropatterned layer because additional layers would deposit homogeneously across the film, as the entire surface is terminated in $-PO_3^{2-}$ after a single iteration.

1-phenylphosphonic, 1-hexylphosphonic, and 1-octadecylphosphonic acids were similarly micropatterned on a fully zirconated substrate. These alkyl or aryl monophosphonates could effectively

block regions of the zirconated substrate such that multilayers of 7 could be built from the remaining zirconated regions. However, the monophosphonates were presumably liberated from the surface upon immersion in a solution of 7/DMSO, as each of these films absorbed enough of 7 to increase at 0.008 absorbance units per layer, and no visible micropatterned film remained. In the highly polar DMSO environment the selective desorption of monophosphonates and subsequent replacement by 7 having multiple points of attachment is not unreasonable.

Further evidence supporting a flattened orientation for 7 was determined through X-ray reflectivity measurements. To demonstrate the utility of a new technique, a test molecule highly characterized in the literature was used. In previous tests, 1,12-Dodecane-bisphosphonic acid, a well-characterized test case, has leaned 35 degrees from perpendicular to the substrate by methods such as ellipsometry.⁴⁴ The model used for fitting the data consisted of a Si substrate, a 2.0 nm SiO₂ layer for the native oxide, and a single slab model for the total multilayer assembly. Multilayers of 1, 2, 3, 4, 6, and 8 layers were grown. Based on a height of 1.9 nm per layer, a 35° lean angle was obtained, in excellent agreement with the literature, thus proving the utility of this technique (Figure 8).

However, when ZPM films of 7 corresponding to 1, 2, 3, 4, 6, and 8 layers were grown and tested by X-ray reflectivity using the same model as detailed above, a similar linear fit is not observed. The initial layers demonstrate a size increase that corresponds to a lean angle of 70° from perpendicular to the substrate. However, the height rapidly increases as a function

of layer after the fourth layer of square is deposited. This is thought to be caused by the strongly charged surface attracting **7** and forcing it into a strained position. The rapid increase in height corresponds to a liberation from the highly constraining surface such that the molecular squares will begin to grow in an upright direction (Figure 9). It is hoped that the problem can be solved by using a spacer with a greater chain length than APTMS.

Conclusions

The successful synthesis and growth of several phosphonate-functionalized molecular squares on both conductive and semiconducting surfaces was demonstrated. The layer-by-layer ZPM growth rate is shown to be uniform by UV-Vis adsorption; however, X-ray reflectivity suggests that the molecular squares adopt a semi-collapsed structure growing straighter as the number of layers increases. Also, the successful observation of a single iteration of the ZPM assembly of the molecular square by both scanning electron microscopy and atomic force microscopy through the MIMIC micropatterning technique was demonstrated.

Despite the fact that **7** adopted semi-collapsed geometry in a ZPM, this research demonstrates the applicability of ZPM synthesis to direct and orient larger molecular assemblies, such as nanoarchitectures, into thin-film assemblies, using molecular structures with cross-sectional areas larger than previously reported. Additionally, this study demonstrates the applicability of XRR measurements to study thin-film assembly by the ZPM technique.

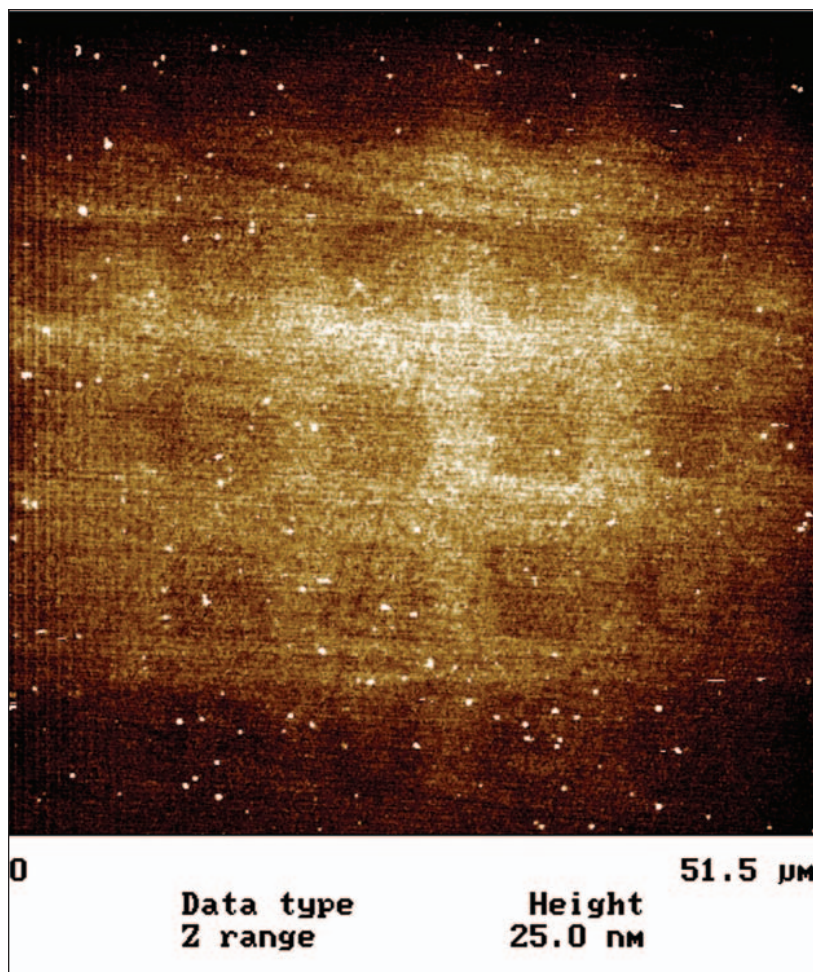


Figure 7: Atomic force micrograph of a single iteration of a ZPM of **7** upon a Zr^{2+} micropatterned phosphorylated ITO-coated glass substrate surface. Micropatterning a single layer of **7** facilitated the observation of the film by AFM.

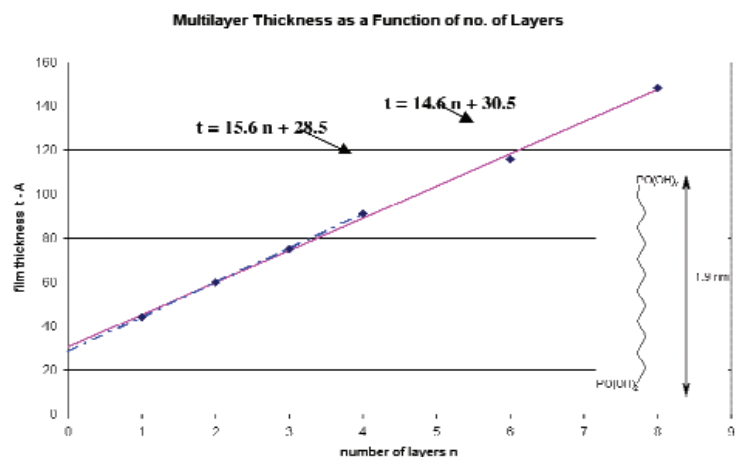


Figure 8: Height as a function of layer for dodecane-bisphosphonic acid, as determined by X-ray reflectivity.

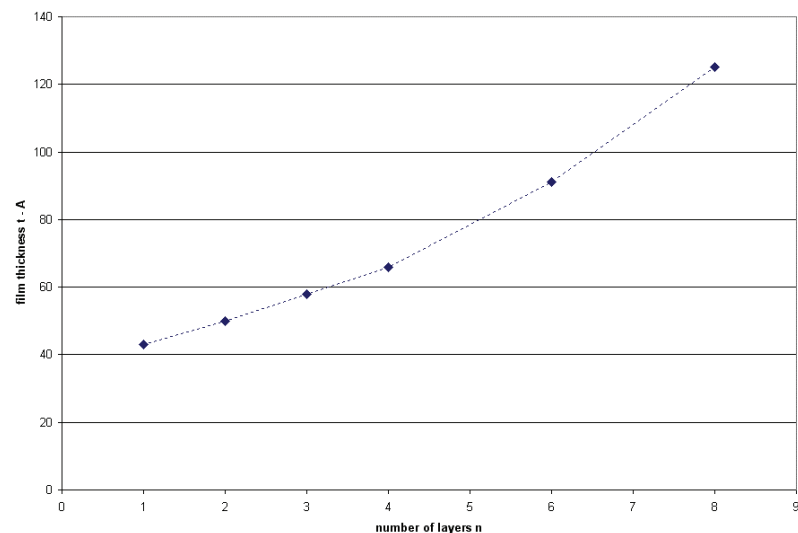


Figure 9: Film thickness as a function of layer, as determined by X-ray reflectivity for 7.

References

- (1) Stix, G. *Scientific American* **1996**, *285*, 32-37.
- (2) Gooding, J. J.; Mearns, F.; Yang, W., et al. *Electroanalysis* **2003**, *15*, 81-96.
- (3) Krausch, G.; Magerle, R. *Adv. Mater.* **2002**, *14*, 1579-83.
- (4) Lehn, J. *Science* **2002**, *295*, 2400-2403.
- (5) Kakkar, A. K. *Chem. Rev.* **2002**, *102*, 3579-87.
- (6) Goldenberg, L. M.; Bryce, M. R.; Petty, M. C. *J. Mater. Chem.* **1999**, *9*, 1957-74.
- (7) Sim, W. S.; Goh, F. Y. *Surf. Rev. Lett.* **2001**, *8*, 491-96.
- (8) Ferreira, M.; Cheung, J. H.; Rubner, M. F. *Thin Solid Films* **1994**, *244*, 806-9.
- (9) Williams, M. E.; Hupp, J. T. *J. Phys. Chem.* **2001**, *B 105*, 8944-50.
- (10) Czaplewski, K. F.; Hupp, J. T.; Snurr, R. Q. *Adv. Mater.* **2001**, *13*, 1895-97.
- (11) Zhang, J.; Williams, M. E.; Keefe, M. H., et al. *Electrochem. Solid-State Lett.* **2002**, *5*, E25-28.
- (12) Merlau, M. L.; Del Pilar Mejia, M.; Nguyen, S. T., et al. *Angew. Chem., Int. Ed. Engl.* **2001**, *40*, 4239-42.
- (13) Mines, G. A.; Tzeng, B.; Stevenson, K. J., et al. *Angew. Chem., Int. Ed. Engl.* **2002**, *41*, 154-57.
- (14) Keefe, M. H.; Benkstein, K. D.; Hupp, J. T. *Coord. Chem. Rev.* **2000**, *205*, 201-28.

-
- (15) Yan, S. G.; Prieskorn, J. S.; Kim, Y., et al. *J. Phys. Chem.* **2000**, *B* **46**, 10871-77.
- (16) Clearfield, A.; Wang, Z. J. *Chem. Soc., Dalton Trans.*, **2002**, *23*, 2937-47.
- (17) Slone, R. V.; Hupp, J. T.; Stern, C. L., et al. *Inorg. Chem.* **1996**, *35*, 4096-97.
- (18) Slone, R. V.; Hupp, J. T. *Inorg. Chem.* **1997**, *36*, 5422-23.
- (19) Slone, R. V.; Benkstein, K. D.; Belanger, S., et al. *Coord. Chem. Rev.* **1998**, *171*, 221-43.
- (20) Keefe, M. H.; Slone, R. V.; Hupp, J. T., et al. *Langmuir* **2000**, *16*, 3964-70.
- (21) Belanger, S.; Stevenson, K. J.; Mudakha, S. A., et al. *Langmuir* **1999**, *15*, 837-43.
- (22) Belanger, S.; Hupp, J. T. *Angew. Chem., Int. Ed. Engl.* **1999**, *38*, 2222-24.
- (23) Belanger, S.; Hupp, J. T.; Stern, C. L., et al. *J. Am. Chem. Soc.* **1999**, *121*, 557-63.
- (24) Williams, M. B.; Stevenson, K. J.; Massari, A. M., et al. *Anal. Chem.* **2000**, *72*, 3122-28.
- (25) Chang, S. H.; Chung, K.-B.; Slone, R. V., et al. *Synth. Met.* **2001**, *117*, 215-17.
- (26) Belanger, S.; Keefe, M. H.; Welch, J. L., et al. *Coord. Chem. Rev.* **1999**, *190-92*, 29-45.
- (27) Cao, G.; Hong, H.-G.; Mallouk, T. E. *Acc. Chem. Res.* **1992**, *25*, 420-27.
- (28) Katz, H. E.; Schilling, M. L.; Chidsey, C. E. D., et al. *Chem. Mater.* **1991**, *3*, 699-703.
- (29) Lee, H.; Kepley, L. J.; Hong, H.-G., et al. *J. Am. Chem. Soc.* **1988**, *110*, 618-20.
- (30) Lee, H.; Kepley, L. J.; Hong, H.-G., et al. *J. Phys. Chem.* **1988**, *92*, 2597-2601.
- (31) Putvinski, T. M.; Schilling, M. L.; Katz, H. E., et al. *Langmuir* **1990**, *6*, 1567-71.
- (32) Clearfield, A. *Progr. Inorg. Chem.* **1998**, *47*, 371-510.
- (33) Byrd, H.; Snover, J. L.; Thompson, M. E. *Langmuir* **1995**, *11*, 4449-53.
- (34) Torsi, L.; Lovinger, A. J.; Crone, B., et al. *J. Phys. Chem.* **2002**, *B* **106**, 12563-68.
- (35) Torsi, L.; Dodabalapur, A.; Rothberg, L. J., et al. *Phys. Rev.* **1998**, *B* **57**, 2271-75.
- (36) Katz, H. E. *Chem. Mater.* **1994**, *6*, 2227-32.
- (37) Katz, H. E.; Wilson, W. L.; Scheller, G. J. *J. Am. Chem. Soc.* **1994**, *116*, 6636-40.
- (38) Katz, H. E.; Scheller, G.; Putvinski, T. M., et al. *Science* **1991**, *254*, 1485-87.
- (39) Zhang, B.; Poojary, M. D.; Clearfield, A. *Inorg. Chem.* **1998**, *37*, 249-54.
- (40) Zhang, B.; Clearfield, A. *J. Am. Chem. Soc.* **1997**, *119*, 2751-52.
- (41) Wu, A.; Talham, D. R. *Langmuir* **2000**, *16*, 7449-56.
- (42) Massari, A. M.; Gurney, R. W.; Huang, S.-H. K., et al. *Polyhedron*, **2003**, in press.
- (43) Horne, J. C.; Huang, Y.; Liu, G. Y., et al. *J. Am. Chem. Soc.* **1998**, *120*, 4419-26.
- (44) Horne, J. C.; Blanchard, G. J. *J. Am. Chem. Soc.* **1998**, *120*, 6336-44.
- (45) Flory, W. C.; Horne, J. C.; Blanchard, G. J. *Biomed. Microdevices* **2001**, *3*, 19-27.
- (46) Kim, E.; Xia, Y. N.; Whitesides, G. M. *J. Am. Chem. Soc.* **1996**, *118*, 5722-31.
- (47) Stevenson, K. J.; Hupp, J. T. *Solid State Lett.* **1999**, *2*, 497-500.
- (48) Katz, H. E.; Schilling, M. L. *Chem. Mater.* **1993**, *5*, 1162-66.
- (49) Zhuravlev, L. T. *Langmuir* **1987**, *3*, 316-18.